

01 Jan 1987

A New Approach to Signal Registration with the Emphasis on Variable Time Delay Estimation

Mohamad Namazi

John A. Stuller

Missouri University of Science and Technology, stuller@mst.edu

Follow this and additional works at: https://scholarsmine.mst.edu/ele_comeng_facwork



Part of the [Electrical and Computer Engineering Commons](#)

Recommended Citation

M. Namazi and J. A. Stuller, "A New Approach to Signal Registration with the Emphasis on Variable Time Delay Estimation," *IEEE Transactions on Acoustics, Speech, and Signal Processing*, vol. 35, no. 12, pp. 1649 - 1660, Institute of Electrical and Electronics Engineers, Jan 1987.

The definitive version is available at <https://doi.org/10.1109/TASSP.1987.1165097>

This Article - Journal is brought to you for free and open access by Scholars' Mine. It has been accepted for inclusion in Electrical and Computer Engineering Faculty Research & Creative Works by an authorized administrator of Scholars' Mine. This work is protected by U. S. Copyright Law. Unauthorized use including reproduction for redistribution requires the permission of the copyright holder. For more information, please contact scholarsmine@mst.edu.

A New Approach to Signal Registration with the Emphasis on Variable Time Delay Estimation

MOHAMAD NAMAZI, MEMBER, IEEE, AND JOHN A. STULLER, SENIOR MEMBER, IEEE

Abstract—Signal registration is concerned with the problem of estimating a varying displacement between two random processes. We approach signal registration here as a recursive demodulation problem in which the recursion is between signal estimations and displacement estimation. Special attention is given to the problem of estimating a variable time delay. Thus, we present new algorithms for estimating $D(t)$ from received processes:

$$r_1(t) = s(t) + n_1(t)$$

$$r_2(t) = s(t - D(t)) + n_2(t)$$

where $s(\cdot)$ is signal and $n_1(\cdot)$ and $n_2(\cdot)$ are noise. Simulation results are presented and discussed.

I. INTRODUCTION

THIS paper presents a novel technique for signal registration. Signal registration can be defined as the problem of estimating a varying displacement between two random processes. This problem has great importance in many applications, perhaps the most familiar of which lies in the field of passive sonar. Here, the bearing of the source signal is related to the time delay (displacement) between two random waveforms [1]. Another application lies in image coding where registration is called "motion estimation." By determining the relative displacement (motion) between the intensities of consecutive image frames, one can encode the image more efficiently [2]. Additional applications exist in geophysics, biomedical engineering, econometric, and the demodulation of nonlinearly modulated waveforms [3].

The approach taken in this paper is to frame the problem of signal registration as an extension of nonlinear modulation theory as described, for example, in the textbook by Van Trees [4].

Modulation theory is concerned with the problem of estimating (demodulating) a random process $D(t)$ from a received waveform

$$r(t) = s(t, D(t)) + n(t) \quad (1)$$

where $n(t)$ is (typically) a sample function from a white Gaussian noise process with spectral density $N_0/2$ and

$s(t, D(t))$ is the modulated waveform. In modulation theory, the function $s(t)$ is usually known. In contrast to the demodulation problem, the registration problem is concerned with estimating a random process $D(t)$ from two received waveforms $r_1(t)$ and $r_2(t)$, where $s(t)$ is a sample function from a random process and where

$$r_1(t) = s(t) + n_1(t) \quad (2a)$$

$$r_2(t) = s(t - D(t)) + n_2(t). \quad (2b)$$

The similarity of (1) and (2) is exploited in the next section, where the basic structure of a new algorithm for estimating $D(t)$ is described.

II. A NEW RECURSIVE ESTIMATOR

Motivation for the algorithm that will be developed in this section can be obtained by first considering a simpler problem in which

$$n_1(t) = 0. \quad (3)$$

Application of (3) in (2a) yields

$$r_1(t) = s(t). \quad (4)$$

Under the assumptions (3) and (4), receiver one receives a replica of the source signal $s(t)$. In this event, (2b) can be interpreted as mapping from $D(t)$ to $r_2(t)$, which is, except for $n_2(t)$, a deterministic mapping. Thus, the assumption $n_1(t) = 0$ reduces the registration problem (2) to the demodulation problem (1) from which $D(t)$ can be recovered by synchronous demodulation.

In the registration problem, $n_1(t)$ is actually not zero. A logical procedure for estimating $D(t)$ is to find an estimate $\hat{s}(t)$ of $s(t)$ from (2a) and to then use $\hat{s}(t)$ in (2b) in order to find an estimate $\hat{D}(t)$ of $D(t)$. Extending this idea, we can then assume that $D(t)$ equals $\hat{D}(t)$ in (2b) and estimate $s(t)$ from the same equation. This procedure can be continued recursively as described below to obtain additional and hopefully improved estimates of $D(t)$ and $s(t)$. To elaborate, let us assume that the estimate of $s(t)$ from (2a) is $\hat{s}^{(1)}(t)$. Then, from (2b), we get

$$r_2(t) = \hat{s}^{(1)}(t - D(t)) + n_2(t) + E_s^{(1)}(t) \quad (5)$$

where

$$E_s^{(1)}(t) = s(t - D(t)) - \hat{s}^{(1)}(t - D(t)). \quad (6)$$

Obviously, $E_s^{(1)}(t)$ results from the error developed in the first estimate of $s(t)$. Now assuming that $E_s^{(1)}(t)$ is small,

Manuscript received April 16, 1986; revised July 9, 1987. This paper includes research submitted by M. Namazi in partial fulfillment of the Ph.D. degree at the University of Missouri, Rolla, MO.

M. Namazi is with the Department of Electrical Engineering, Michigan Technological University, Houghton, MI 49931.

J. A. Stuller is with the Department of Electrical Engineering, University of Missouri, Rolla, MO 65401.

IEEE Log Number 8717263.

we obtain the first estimate of $D(t)$, $\hat{D}^{(1)}(t)$, from (5). We proceed by assuming that $D(t) \approx \hat{D}^{(1)}(t)$ and obtain a second estimate of $s(t)$ from (2b) as follows:

$$\begin{aligned} r_2(t + \hat{D}^{(1)}(t)) &= s(t - D(t) + \hat{D}^{(1)}(t)) \\ &+ n_2(t + \hat{D}^{(1)}(t)) \approx s(t) \\ &- E_D^{(1)}(t) \frac{\partial s(t)}{\partial t} + n_2^{(1)}(t) \end{aligned} \quad (7)$$

where

$$E_D^{(1)}(t) = D(t) - \hat{D}^{(1)}(t) \quad (8)$$

and

$$n_2^{(1)}(t) = n_2(t + \hat{D}^{(1)}(t)). \quad (9)$$

Hence, from (7), it follows that

$$r_2(t + \hat{D}^{(1)}(t)) = s(t) + n_2^{(1)}(t). \quad (10)$$

From (10) we obtain the second estimate of $s(t)$, denoted by $\hat{s}^{(2)}(t)$. Then,

$$r_2(t) = \hat{s}^{(2)}(t - D(t)) + n_2(t) + E_s^{(2)}(t) \quad (11)$$

where

$$E_s^{(2)}(t) = s(t - D(t)) - \hat{s}^{(2)}(t - D(t)). \quad (12)$$

$\hat{D}^{(2)}(t)$ is obtained from (11) assuming that $E_s^{(2)}(t) \approx 0$. Continuation of this process results in a recursive scheme in which we generate the sequence of estimates $\{\hat{s}^{(1)}(t), \hat{D}^{(1)}(t), \hat{s}^{(2)}(t), \dots\}$. A simplified version of the process is depicted by Fig. 1 in which $r_1(t)$ and $r_2(t)$ are assumed to be prerecorded over some finite time interval $T = [T_i, T_f]$.

Thus far, we have not specified the estimation criterion. The maximum *a posteriori* (MAP) probability criterion, maximum likelihood (ML) criterion, and minimum mean square error (MMSE) criterion are considered in subsequent sections.

III. ESTIMATION BASED ON MAP CRITERION

In this section, we apply the MAP criterion to the iterative scheme introduced in the preceding section.

To help us in finding the estimates of $s(t)$ and $D(t)$, let us consider the following equation:

$$r(t) = s(t, a(t)) + n(t) \quad T_i \leq t \leq T_f \quad (13)$$

where $n(t)$ is a sample function from a zero-mean white Gaussian process and $a(t)$ is a sample function from a zero-mean Gaussian process. Also assume that $s(t)$ is a known voltage function and $s(t, a(t))$ is differentiable with respect to $a(t)$.

The MAP estimate of $a(t)$ is obtained by solving the integral equation [4]

$$\begin{aligned} \hat{a}(t) &= \frac{2}{N_o} \int_{T_i}^{T_f} K_a(t, z) \frac{\partial s(z, \hat{a}(z))}{\partial \hat{a}(z)} \\ &\cdot [r(z) - s(z, \hat{a}(z))] dz \quad T_i \leq t \leq T_f \end{aligned} \quad (14)$$

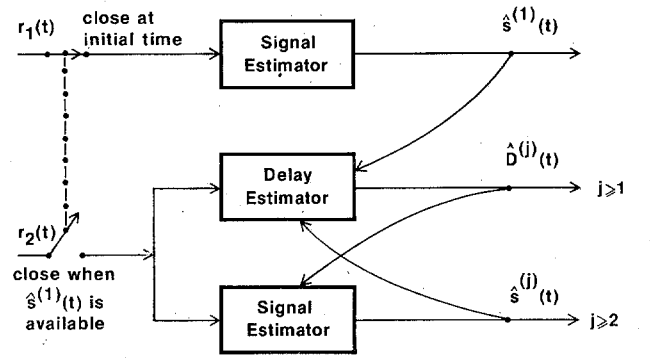


Fig. 1. Structure of the recursive estimation scheme ($r_1(t)$ and $r_2(t)$ are prerecorded over $[T_i, T_f]$).

where $K_a(t, z)$ is the covariance function of $a(t)$, and $N_o/2$ is the two-sided spectral density of $n(t)$.

Equation (14) can be readily related to our problem by proper choice of functions. Substitution of $s(t, a(t)) = a(t)$, $r(t) = r_1(t)$, $a(t) = s(t)$, $K_a(t, z) = K_s(t, z)$, and $N_o = N_{o1}$ in (14) results in the estimate of $s(t)$ as follows:

$$\begin{aligned} \hat{s}(t) &= \frac{2}{N_{o1}} \int_{T_i}^{T_f} K_s(t, z) [r_1(z) - \hat{s}(z)] dz \\ T_i &\leq t \leq T_f \end{aligned} \quad (15)$$

where $K_s(t, z)$ is the covariance function of $s(t)$, and $N_{o1}/2$ is the power spectral density of $n_1(t)$. Accordingly, $s(t, a(t)) = s(t - a(t))$, $r(t) = r_2(t)$, $a(t) = D(t)$, $K_a(t, z) = K_D(t, z)$, and $N_o = N_{o2}$ in (14) leads to the delay equation

$$\begin{aligned} \hat{D}(t) &= \frac{2}{N_{o2}} \int_{T_i}^{T_f} K_D(t, z) \frac{\partial s(z - \hat{D}(z))}{\partial \hat{D}(z)} \\ &\cdot [r_2(z) - s(z - \hat{D}(z))] dz \quad T_i \leq t \leq T_f \end{aligned} \quad (16)$$

where $K_D(t, z)$ is the covariance function of $D(t)$, and $N_{o2}/2$ is the power spectral density of $n_2(t)$. Equation (16) can be written in a form which is more suitable for simulation. Using chain rule, we have

$$\frac{\partial s(z - \hat{D}(z))}{\partial \hat{D}(z)} = - \frac{\partial s(z - \hat{D}(z))}{\partial (z - \hat{D}(z))}. \quad (17)$$

Application of (17) in (16) yields

$$\begin{aligned} \hat{D}(t) &= - \frac{2}{N_{o2}} \int_{T_i}^{T_f} K_D(t, z) \frac{\partial s(z - \hat{D}(z))}{\partial (z - \hat{D}(z))} \\ &\cdot [r_2(z) - s(z - \hat{D}(z))] dz \quad T_i \leq t \leq T_f. \end{aligned} \quad (18)$$

As stated in the previous section, the estimate $\hat{s}^{(1)}(t)$ can be obtained using the waveform received at the first receiver (15), and the delay estimate $\hat{D}^{(1)}(t)$ can be obtained

using the signal received at the second receiver assuming that $s(t) = \hat{s}^{(1)}(t)$ (18).

Therefore,

$$\hat{s}^{(1)}(t) = \frac{2}{N_{01}} \int_{T_i}^{T_f} K_s(t, z) [r_1(z) - \hat{s}^{(1)}(z)] dz \quad (19)$$

and

$$\begin{aligned} \hat{D}^{(1)}(t) = & -\frac{2}{N_{02}} \int_{T_i}^{T_f} K_D(t, z) \frac{\partial \hat{s}^{(1)}(z - \hat{D}^{(1)}(z))}{\partial (z - \hat{D}^{(1)}(z))} \\ & \cdot [r_2(z) - \hat{s}^{(1)}(z - \hat{D}^{(1)}(z))] dz. \end{aligned} \quad (20)$$

From (10) and (15) we get

$$\begin{aligned} \hat{s}^{(2)}(t) = & \frac{2}{N_{02}} \int_{T_i}^{T_f} K_s(t, z) [r_2(z + \hat{D}^{(1)}(z)) \\ & - \hat{s}^{(2)}(z)] dz \quad T_i \leq t \leq T_f \end{aligned} \quad (21)$$

where, for simplicity, we have assumed that $n_2^{(1)}(t)$ and $n_2(t)$ have the same statistics. Continuation of this process with the assumption $n_2^{(i)}(t)$, $i = 2, 3, \dots$, and $n_2(t)$ are statistically equivalent results in the sequence $\{\hat{s}^{(1)}(t), \hat{D}^{(1)}(t), \dots\}$. The algorithm is shown in Fig. 2 where it is referred to as Algorithm 1. It should be noted that the first receiver only serves as an initializer from which the loop starts. Therefore, it is logical to keep the less contaminated receiver inside the loop and initialize the algorithm by the "noisier" receiver. This approach worked best for the simulation experiments we attempted.

IV. SIMULATION EXPERIMENT USING ALGORITHM 1

This section describes the results of two sets of experiments involving Algorithm 1. Experiment 1 is in the category of linear signaling (linear modulation), and Experiment 2, more suitable for a known source signal, treats the case for which $D(t)$ is assumed to be a sample function from a white Gaussian process. All experiments described in this paper were performed by digital simulation. Thus, $t = ih$, where h is the sampling interval and $i = 1, 2, 3, \dots$.

Experiment 1: In this experiment, the source signal and the delay waveform are both assumed to be sample functions from ramp processes with slopes a and b , respectively, where a and b are zero mean, Gaussian random variables with variances σ_a^2 and σ_b^2 , respectively. The receiver equations are

$$r_1(t) = at + n_1(t) \quad (22a)$$

$$r_2(t) = a(1 - b)t + n_2(t) \quad (22b)$$

where $t = ih$, $i = 1, 2, 3, \dots$. Application of (22) in Algorithm 1 results in the Algorithm 1A shown by Fig. 3. Figs. 4 and 5 illustrate typical simulation results wherein the random variable a has variance of $2(v/s)^2$, and b has variance of 2; $n_1(ih)$ and $n_2(ih)$ are independent white Gaussian noise sequences with variances $N_{01}/2h = 100 v^2$ and $N_{02}/2h = 0.1 v^2$, respectively.

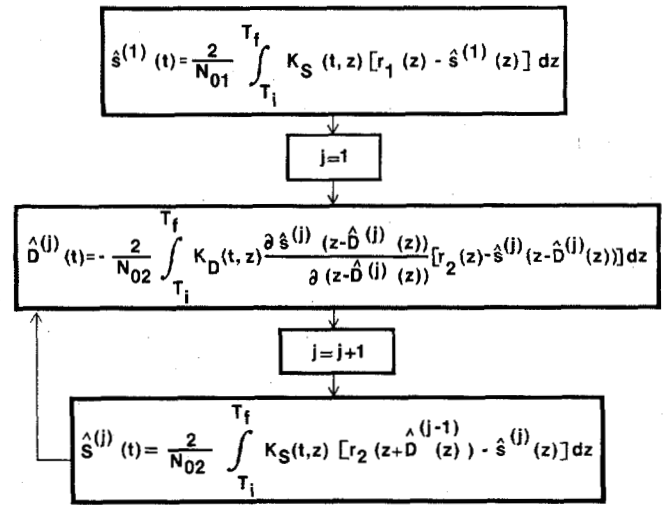


Fig. 2. Algorithm 1.

This corresponds to band-limited white noise sampled at Nyquist rate. The sampling time h is 0.005 s. Integration times T are 0.75 s and 0.25 s, respectively, in Figs. 4 and 5. Note that for each of these simulations, the estimation error tends to decrease with increasing iterations. As would be expected, steady-state error is smaller and is reached more quickly for larger T . In Fig. 6, $n_1(ih)$ and $n_2(ih)$ have $N_{01}/2h = 0.1 v^2$ and $N_{02}/2h = 10 v^2$, respectively. The integration time T is 0.4 s and a and b have variances of $2(v/s)^2$ and 2, respectively. This simulation illustrates the discussion of the previous section. The estimation error is seen to increase rapidly following the first estimate due to the relatively large amount of noise in the feedback loop.

Experiment 2: In this experiment, $D(t)$ is modeled as a sample function from a white Gaussian process. Thus,

$$K_D(t, z) = Q_o/2 \delta(t - z) \quad (23)$$

where $Q_o/2$ is spectral density of $D(t)$. We restrict our attention in this experiment to the case in which $s(t)$ is known. Using the covariance function (23), (18) simplifies to

$$\begin{aligned} \hat{D}(t) = & -\frac{Q_o}{N_{02}} \frac{\partial s(t - \hat{D}(t))}{\partial (t - \hat{D}(t))} \\ & \cdot [r_2(t) - s(t - \hat{D}(t))] \quad T_i \leq t \leq T_f, \end{aligned} \quad (24)$$

or equivalently,

$$\hat{D}_j = -\frac{Q_o}{N_{02}} \frac{\partial s(t_j - \hat{D}_j)}{\partial (t_j - \hat{D}_j)} [r_2(t_j) - s(t_j - \hat{D}_j)] \quad (25)$$

where

$$\hat{D}_j \triangleq \hat{D}(t_j). \quad (26)$$

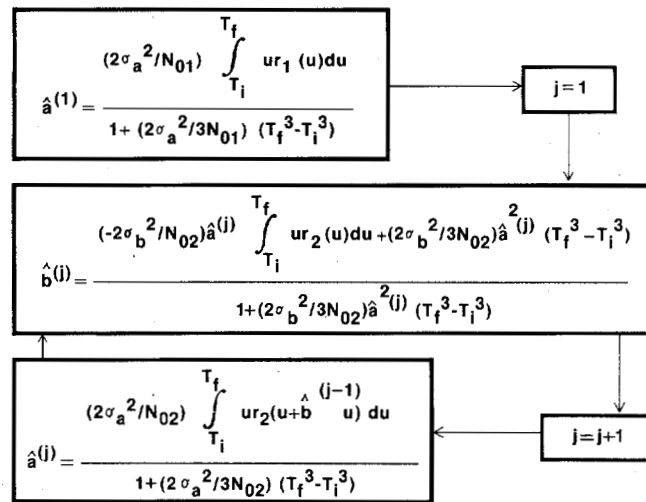
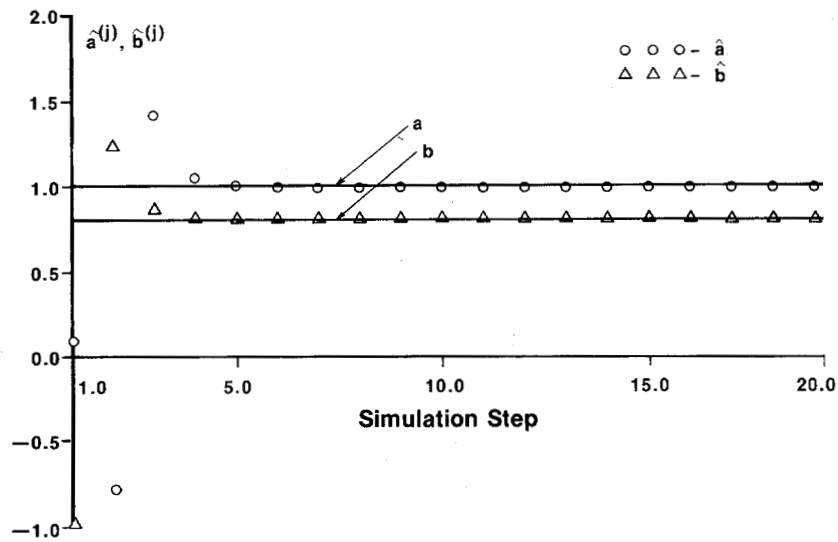
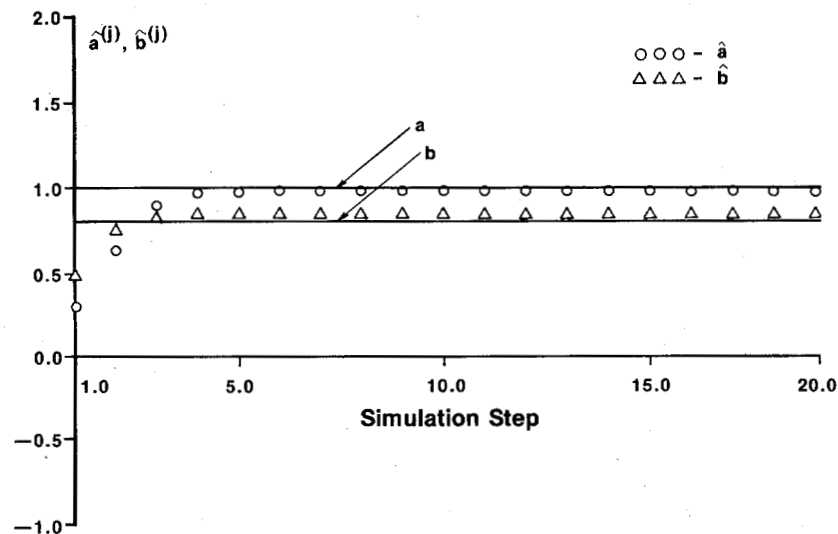


Fig. 3. Algorithm 1A.

Fig. 4. Estimates of the slopes of $s(t)$ and $D(t)$ ($\hat{a}^{(j)}$ and $\hat{b}^{(j)}$, respectively) using Algorithm 1A with $N_{01}/2h = 100 v^2$, $N_{02}/2h = 0.1 v^2$, $\sigma_a^2 = 2 (v/s)^2$, $\sigma_b^2 = 2$, $T = 0.75$ s, and $h = 0.005$ s.Fig. 5. Estimates of the slopes of $s(t)$ and $D(t)$ ($\hat{a}^{(j)}$ and $\hat{b}^{(j)}$, respectively) using Algorithm 1A with $N_{01}/2h = 100 v^2$, $N_{02}/2h = 0.1 v^2$, $\sigma_a^2 = 2 (v/s)^2$, $\sigma_b^2 = 2$, $T = 0.25$ s, and $h = 0.005$ s.

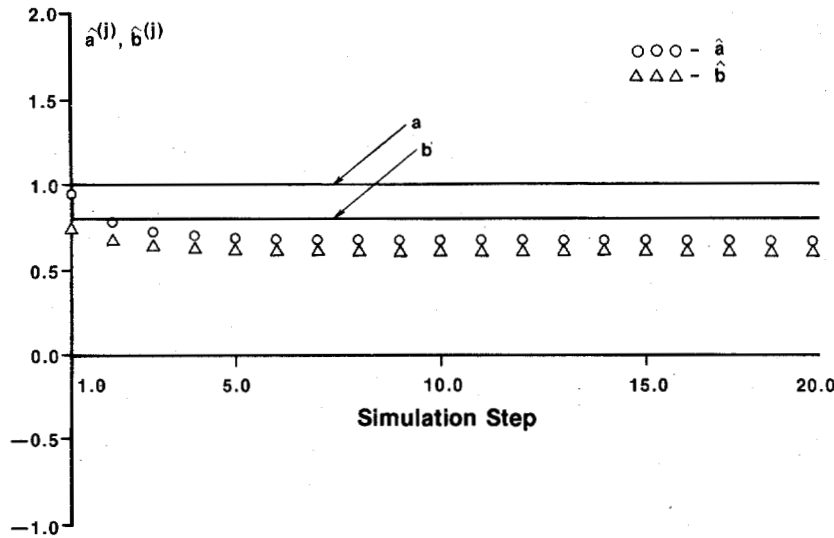


Fig. 6. Estimates of the slopes of $s(t)$ and $D(t)$ ($\hat{a}^{(j)}$ and $\hat{b}^{(j)}$, respectively) using Algorithm 1A with $N_{01}/2h = 0.1 v^2$, $N_{02}/2h = 10 v^2$, $\sigma_a^2 = 2 (v/s)^2$, $\sigma_b^2 = 2$, $T = 0.4$ s, and $h = 0.005$ s.

In order to solve (25) for \hat{D}_j , we define a “null function”

$$N_j(y) \triangleq y + \frac{Q_o}{N_{02}} \frac{\partial s(t_j - y)}{\partial (t_j - y)} \cdot [r_2(t_j) - s(t_j - y)] \quad j = 1, 2, \dots, K. \quad (27)$$

The roots of the equation

$$N_j(y) = 0 \quad j = 1, 2, \dots, k \quad (28)$$

are the MAP estimates \hat{D}_j , $j = 1, 2, \dots, k$. It should be noted that $N_j(y)$ can have more than one root for each $j = 1, 2, \dots, k$, [5].

A simple procedure for solving (28) is to increment y in $N_j(y)$ by integer multiples of h beginning with $y = -\alpha$ increasing toward $+\alpha$. The estimate $\hat{D}(t_j)$ is taken to be the first value of y causing $N_j(y)$ to change sign. This process is shown by the flowchart in Fig. 7. The above approach was applied to the sinusoidal source and delay waveforms shown by Figs. 8 and 9. The search range 2α was chosen as 1.001 s and the noise variance $N_{02}/2h = 0.01 v^2$. This experiment was examined over 1.575 s with $h = 0.0007$ s and delay variance $Q_o/2h = 0.04 s^2$. The delay estimation error, $e(t) = D(t) - \hat{D}(t)$, is shown by Fig. 10. Note that the null function (27) will be independent of the data if the source signal has zero derivative. This fact justifies the anomalies seen by Fig. 10 over the slow varying region of $s(t)$.

Simulation experiments have shown that (24) can also be applied for nonwhite and non-Gaussian delay waveforms. For example, using a random step delay signal and the known sinusoidal source signal shown by Fig. 8(a), we obtain results shown by Fig. 11. As explained before,

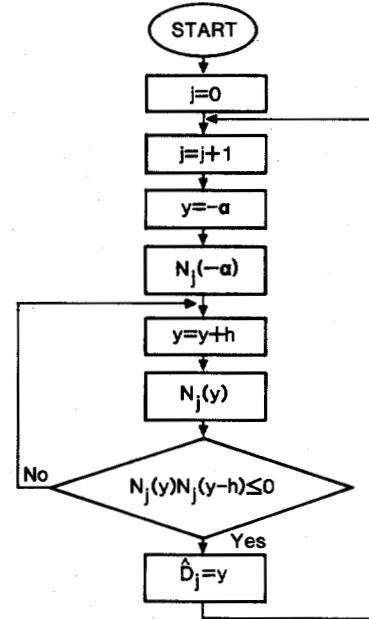


Fig. 7. Flowchart of algorithm used to solve (27).

the estimator exhibits some anomalies over the region for which $s(t)$ is slowly varying. The “clean ramp” portion of $\hat{D}(t)$ results from the numerical procedure for solving (28) with near zero signal derivative.

V. ESTIMATION BASED ON THE ML CRITERION

This section describes an adaptive estimator based on the ML criterion.

Here we consider $s(t)$ and $a(t)$ in (13) to be sample functions from zero-mean processes with covariance functions $k_s(t, u)$ and $k_D(t, u)$, respectively, but whose statistics are otherwise unknown. We represent $a(t)$ as Fourier series expansion

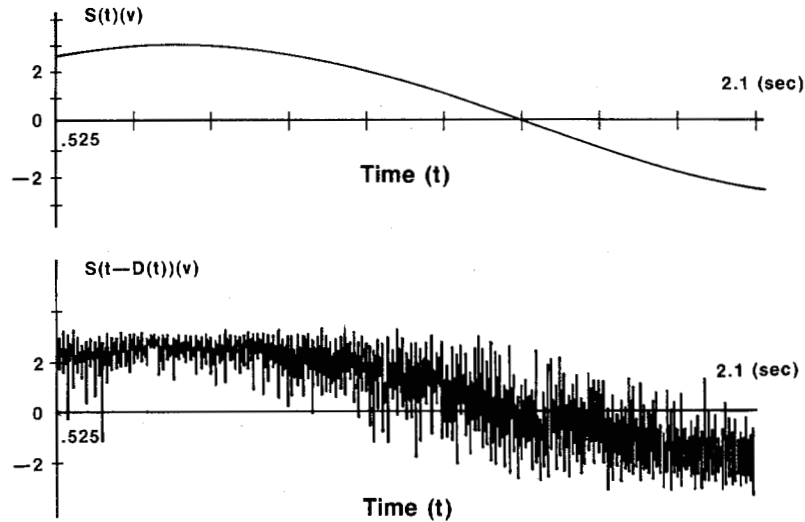


Fig. 8. (a) Assumed known source signal with $a = 3 v$ and $w = 2 \text{ rad/s}$.
(b) Delayed version of the source signal shown in (a) with "white" delay shown in Fig. 9.

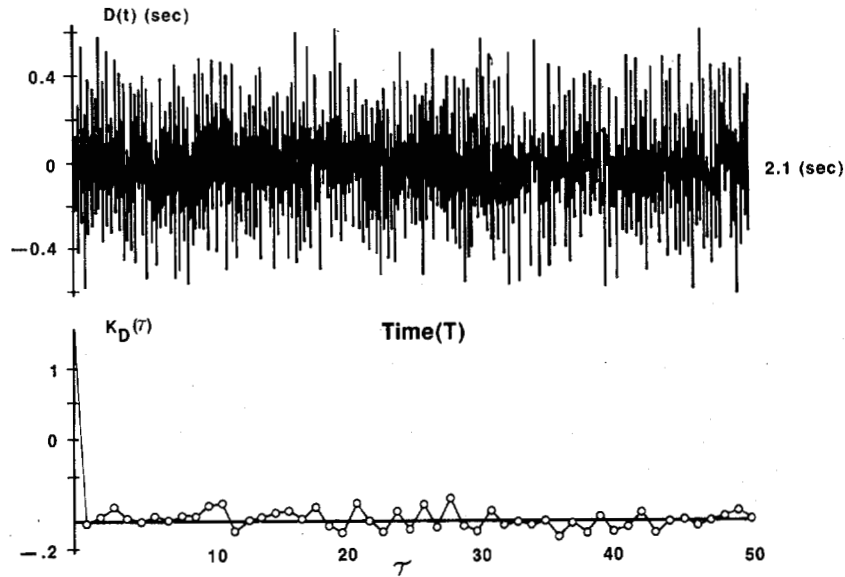


Fig. 9. (a) A sampled function of a computer generated "white" sequence with $Q_o/2h = 0.04 \text{ s}^2$. (b) Estimate of normalized autocorrelation function of the process shown in (a).

$$a_k(t) = \sum_{i=1}^k a_i \psi_i(t) \quad (29)$$

where $k \rightarrow \infty$.

We choose the $\psi_i(t)$ to be the normalized eigenfunction solutions of

$$\mu_i \psi_i(t) = \int_{T_i}^{T_f} K_a(t, u) \psi_i(u) du \quad (30)$$

and μ_i is the corresponding eigenvalues. The coefficients are

$$a_i = \int_{T_i}^{T_f} a(t) \psi_i(t) dt. \quad (31)$$

Then $s(t, a(t))$ is equivalent to $s(t, \mathbf{a})$ in which $\mathbf{a} = (a_1, a_2, \dots, a_k)^T$.

For additive white Gaussian noise as in (13), the maximum likelihood estimate of \mathbf{a} is the vector $\mathbf{A} = (A_1, A_2, \dots, A_K)^T$ maximizing the log likelihood function [4]

$$\ln \Lambda_1[r(t), \mathbf{A}] = \frac{2}{N_O} \int_{T_i}^{T_f} r(t) s(t, \mathbf{A}) dt - \frac{1}{N_O} \int_{T_i}^{T_f} s^2(t, \mathbf{A}) dt. \quad (32)$$

Application of steepest ascent algorithm to (32) yields

$$\hat{A}_i(n) = \hat{A}_i(n-1) + \frac{\epsilon_i}{2} \frac{\partial}{\partial A_i} \ln \Lambda_1[r(t), \mathbf{A}] \Big|_{\hat{A}_i(n-1)} \quad (33)$$

for $i = 1, 2, \dots, K$, in which the parameter ϵ_i is chosen to influence the rate of convergence. The substitution of

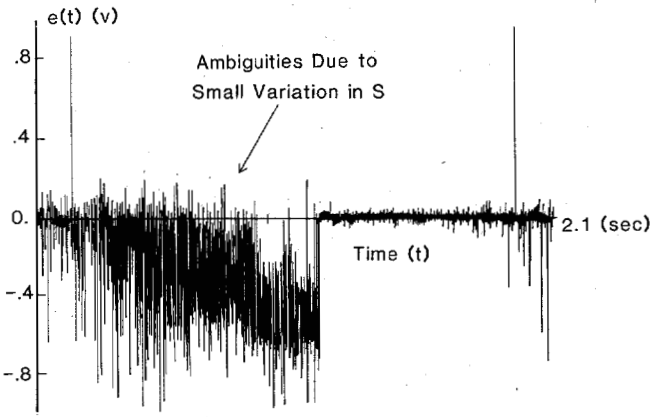


Fig. 10. Estimation error of the delay process shown by Fig. 9(a) using (27) with $N_{02}/2h = 0.01 \text{ v}^2$.

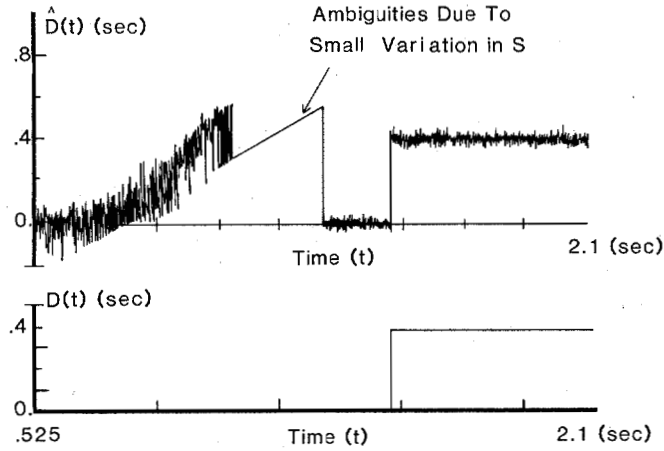


Fig. 11. Non-“white” delay estimation using (27) with $N_{02}/2h = 0.01 \text{ v}^2$ and $Q_{02}/2h = 0.04 \text{ s}^2$. (a) Delay estimate, (b) actual delay.

(32) and (33) yields

$$\begin{aligned} \hat{A}_i(n) = & \hat{A}_i(n-1) + \frac{\epsilon_i}{N_O} \int_{T_i}^{T_f} \\ & \cdot [r(z) - s(z, \hat{A}(n-1))] \\ & \cdot \frac{\partial s(z, \hat{A})}{\partial \hat{A}_i} \bigg|_{\hat{A}(n-1)} dz, \end{aligned} \quad (34)$$

or equivalently,

$$\begin{aligned} \hat{A}_i(n) = & \hat{A}_i(n-1) + \frac{\epsilon_i}{N_O} \int_{T_i}^{T_f} \\ & \cdot [r(z) - s(z, \hat{A}(n-1))] \\ & \cdot \frac{\partial s(z, a_K(z))}{\partial a_K(z)} \bigg|_{\hat{a}_K(z, n-1)} \psi_i(z) dz \end{aligned} \quad (35)$$

in which

$$\hat{a}_K(t, n) = \sum_{i=1}^K \hat{A}_i(n) \psi_i(t). \quad (36)$$

Further combination of (35) and (36) with

$$\epsilon_i = \epsilon \mu_i \quad (37)$$

yields

$$\begin{aligned} \hat{a}_K(t, n) = & \hat{a}_K(t, n-1) + \frac{\epsilon}{N_O} \int_{T_i}^{T_f} \\ & \cdot [r(z) - s(z, \hat{a}(z, n-1))] \\ & \cdot \frac{\partial s(z, a_K(z))}{\partial a_K(z)} \bigg|_{\hat{a}_K(z, n-1)} \\ & \cdot \sum_{i=1}^K \mu_i \psi_i(t) \psi_i(z) dz. \end{aligned} \quad (38)$$

By taking the limit $K \rightarrow \infty$ with

$$\hat{a}(t, n) = \lim_{K \rightarrow \infty} \sum_{i=1}^K \hat{A}_i(n) \psi_i(t) \quad (39)$$

and invoking Mercer's theorem [4] we have

$$K_a(t, z) = \lim_{K \rightarrow \infty} \sum_{i=1}^K \mu_i \psi_i(t) \psi_i(z). \quad (40)$$

Then, (38) becomes, finally,

$$\begin{aligned} \hat{a}_n(t) = & \hat{a}_{n-1}(t) + \frac{\epsilon}{N_O} \\ & \cdot \int_{T_i}^{T_f} K_a(t, z) \frac{\partial s(z, a(z))}{\partial a(z)} \bigg|_{\hat{a}_{n-1}(z)} \\ & \cdot [r(z) - s(z, \hat{a}_{n-1}(z))] dz. \end{aligned} \quad (41)$$

For delay estimation (41) becomes

$$\begin{aligned} \hat{D}_m(t) = & \hat{D}_{m-1}(t) - \frac{\epsilon_2}{N_{O2}} \\ & \cdot \int_{T_i}^{T_f} K_D(t, z) \frac{\partial s(z - \hat{D}_{m-1}(z))}{\partial (z - \hat{D}_{m-1}(z))} \\ & \cdot [r_2(z) - s(z - \hat{D}_{m-1}(z))] dz \end{aligned} \quad (42)$$

and for signal estimation (41) becomes

$$\begin{aligned} \hat{s}_n(t) = & \hat{s}_{n-1}(t) + \frac{\epsilon_1}{N_{O1}} \int_{T_i}^{T_f} K_s(t, z) \\ & \cdot [r_1(z) - \hat{s}_{n-1}(z)] dz. \end{aligned} \quad (43)$$

Following the same procedure that led to Algorithm 1, we obtain an alternative algorithm called Algorithm 2 (Fig. 12).

Notice that the above estimates $\hat{s}_n(t)$ and $\hat{D}_m(t)$ are not ML estimates in the conventional sense because they assume knowledge of the signal and delay covariance functions $K_s(t, z)$ and $K_D(t, z)$, respectively. However, they make no additional assumptions regarding the statistics of $s(t)$ and $D(t)$. Since they use the ML estimates of Karhunen-Loève expansion coefficients, (42) and (43) are based on the ML criterion. The exact theoretical solution

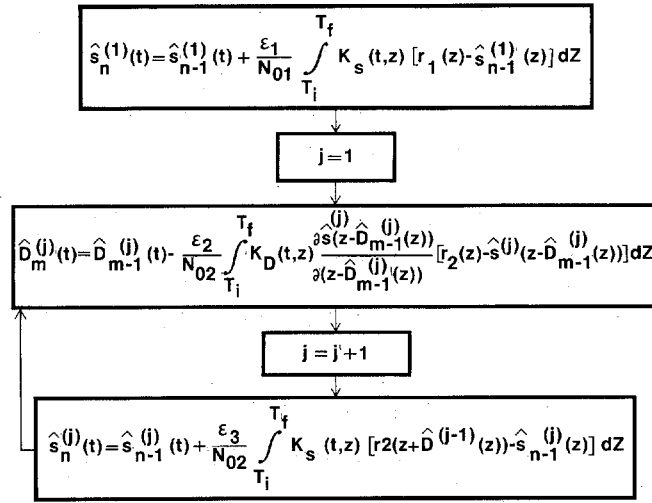


Fig. 12. Algorithm 2.

to the problem of ML estimation of time-varying delay appears in [9].

As seen from Algorithm 2, Fig. 12, (43) requires an initial estimate $\hat{s}_0(t)$, for the whole interval $t \in [T_i, T_f]$. We take $\hat{s}_0(t) \equiv 0$ for $t \in [T_i, T_f]$ because $s(t)$ is zero mean. The resulting estimate $\hat{s}^{(j)}(t)$ (after a sufficient iteration in n) is used in the second equation to find the delay estimate. Equation (42) also requires the initial values

$$\hat{D}_0^{(j)}(t), \frac{\partial \hat{s}^{(j)}(t - \hat{D}_0^{(j)}(t))}{\partial (t - \hat{D}_0^{(j)}(t))}$$

and $\hat{s}^{(j)}(t - \hat{D}_0^{(j)}(t))$

$j = 1, 2, \dots$. The most reasonable choice for $\hat{D}_0^{(j)}(t)$ is zero, since in this manner we have

$$\frac{\partial \hat{s}^{(j)}(t - \hat{D}_0^{(j)}(t))}{\partial (t - \hat{D}_0^{(j)}(t))} = \frac{\partial \hat{s}^{(j)}(t)}{\partial t} \quad (44)$$

and

$$\hat{s}^{(j)}(t - \hat{D}_0^{(j)}(t)) = \hat{s}^{(j)}(t) \quad (45)$$

where $\hat{s}^{(j)}(t)$ is available from the previous step of the algorithm, and $\partial \hat{s}^{(j)}(t) / \partial t$ can be evaluated using the definition of the derivative or four-point difference algorithm [8]. The whole process is illustrated by the flowchart shown by Fig. 13.

Finally, for the cases for which $D(t)$ is a sample function from a stationary random process, (42) can be approximated as follows:

$$\begin{aligned} \hat{D}_m(t) &\approx \hat{D}_{m-1}(t) - \frac{\epsilon_2}{N_{02}} \\ &\cdot \int_{t-l\tau_D}^{t+l\tau_D} K_D(t-z) \frac{\partial s(z - \hat{D}_{m-1}(z))}{\partial (z - \hat{D}_{m-1}(z))} \\ &\cdot [r_2(z) - s(z - \hat{D}_{m-1}(z))] dz \end{aligned} \quad (46)$$

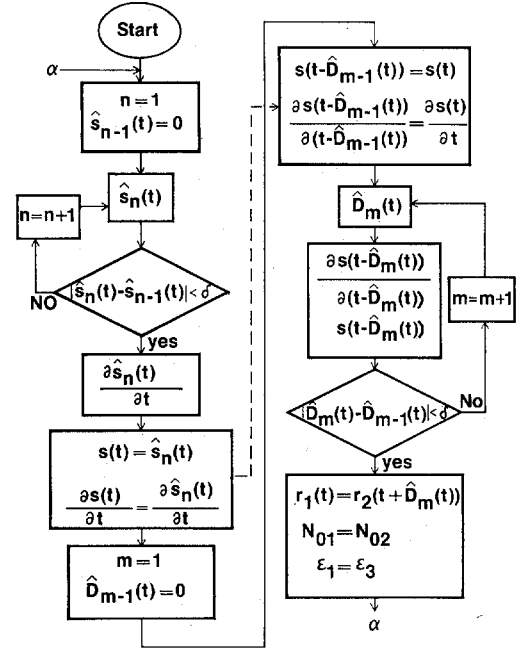


Fig. 13. Flowchart of Algorithm 2.

where τ_D is the correlation time of $D(t)$ and l is an appropriate positive integer depending on the correlation coefficient of $D(t)$. Notice that this case results in a significant reduction in computational time of the algorithm.

VI. SIMULATION EXPERIMENT USING ALGORITHM 2

We describe two sets of simulation experiments using the recursive Algorithm 2. The source signal in all experiments is modeled as a sample function from a sinusoidal process with random amplitude a :

$$s(t) = a \sin \omega t \quad (47)$$

where ω is assumed to be 10 rad/s and the random variable a has a variance $49 v^2$. A sample function of $s(t)$ used in the following experiments is shown by Fig. 14. The samples of the delay waveform in Experiment 3 are modeled as Markov-1 sequence and Experiment 4 investigates the case for which $D(t)$ is linearly varying. In all cases, the derivatives $d\hat{s}/dt$ appearing in Algorithm 2 were computed numerically using the four-point difference algorithm [8].

Experiment 3: In this experiment, samples of $D(t)$ are modeled as a discrete stationary Markov-1 random sequence:

$$\begin{aligned} D(1) &= \xi W(1) \\ D(n) &= \rho D(n-1) + W(n) \end{aligned} \quad (48)$$

where ρ is correlation coefficient of the sequence

$$\xi = \frac{1}{1 - \rho^2}; \quad \sigma_D^2 = \left(\frac{1}{1 - \rho^2} \right) \sigma_W^2 \quad (49)$$

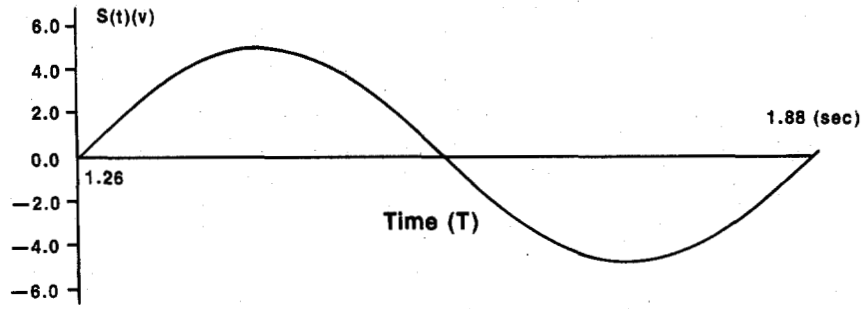


Fig. 14. A sample function of the source signal with $a = 5 \text{ v}$ and $w = 10 \text{ rad/s}$.

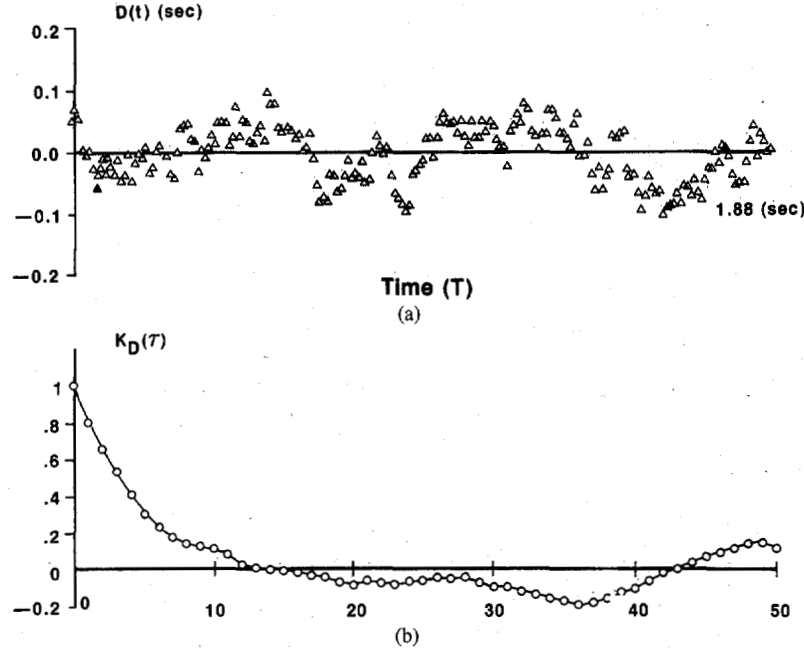


Fig. 15. (a) A sample function from the Markov-1 sequence generated by (48) with $\rho = 0.85$ and $\sigma_D^2 = 0.001 \text{ s}^2$. (b) Estimate of normalized autocorrelation function of the process shown in (a).

and $\{W_n\}$ is a white sequence with variance σ_w^2 . A sample function from this process along with its estimated covariance function is shown by Fig. 15.

Simulation results showed that for signal estimation it suffices to iterate each point 20 times ($n = 20$), and for delay estimation it is required to iterate 50 times ($m = 50$).

When the power spectrum of $n_1(t)$ and $n_2(t)$ are low enough, only one iteration in J may be sufficient. This case was examined for $N_{O1}/2h = N_{O2}/2h = 0.001 \text{ v}^2$, $a = 5 \text{ v}$, $\epsilon_1 = 6 \times 10^{-8}$, and $\epsilon_2 = 6 \times 10^{-4}$. The delay estimation error is shown by Fig. 16(a). Fig. 16(b) illustrates the final delay estimation error for noisier situation. In this case, $N_{O1}/2h = 10^5 \text{ v}^2$, $N_{O2}/2h = 0.1 \text{ v}^2$, $a = 2 \text{ v}$, $\epsilon_1 = 6$, $\epsilon_2 = 6 \times 10^{-2}$, and $\epsilon_3 = 6 \times 10^{-6}$. The algorithm converges after three iterations in J . In both experiments, $\rho = 0.85$, $h = 0.0031 \text{ s}$, and $\sigma_D^2 = 0.001 \text{ s}^2$.

Experiment 4: In this experiment, the delay waveform is a sample function from a ramp process with random slope b

$$D(t) = bt. \quad (50)$$

Fig. 17 illustrates $\hat{s}_{20}^{(j)}(t)$ and $\hat{D}_{50}^{(j)}(t)$ for $a = 5 \text{ v}$, $\sigma_a^2 = 49 \text{ v}^2$, $b = 0.15$, $\sigma_b^2 = 0.05$, $N_{O1}/2h = 100 \text{ v}^2$, $N_{O2}/2h = 0.01 \text{ v}^2$, $h = 0.0031 \text{ s}$, $\epsilon_1 = 6 \times 10^{-6}$, $\epsilon_2 = 6 \times 10^{-6}$, and $\epsilon_3 = 3 \times 10^{-6}$.

VII. ESTIMATION BASED ON MMSE CRITERION

As a final algorithm, we present an adaptive estimator that searches for the values of $a(t)$ in

$$r(t) = s(t, a(t)) \quad (51)$$

such that $E\{e^2(t)\}$ is minimum, where

$$e(t) \triangleq s(t, a(t)) - s(t, \hat{a}(t)) \quad (52)$$

and $s(t)$ is assumed to be known and differentiable with respect to $a(t)$. The preliminary steps of derivations are parallel to Etter and Stearns [7] who developed a similar technique suitable for sampled data systems.

Using the conventional search method, we can write

$$\hat{a}_n(t) = \hat{a}_{n-1}(t) - \frac{\mu}{2} \frac{\partial}{\partial \hat{a}_{n-1}(t)} [E\{e^2(t)\}]. \quad (53)$$

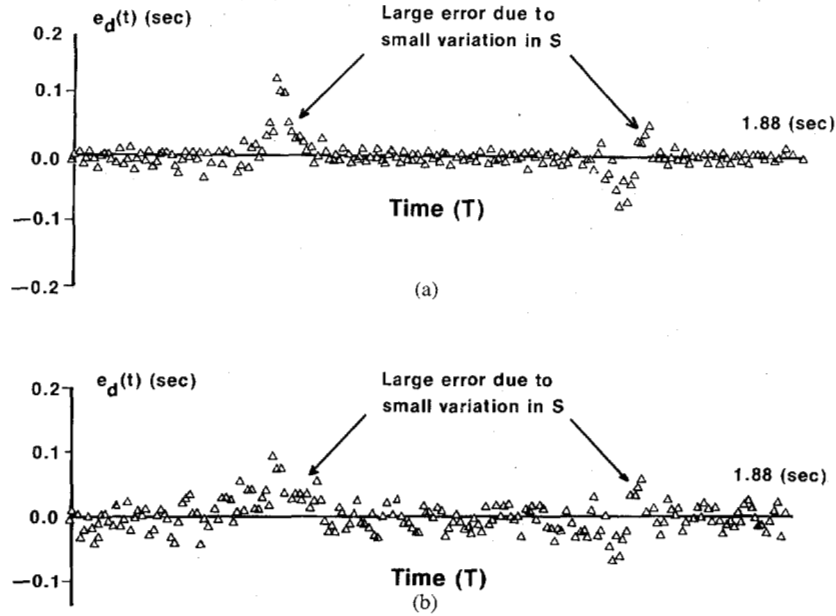


Fig. 16. Estimation of the delay process shown in Fig. 15(a) using Algorithm 2 with: (a) $N_{01}/2h = N_{02}/2h = 0.001 v^2$, $a = 5 v$, $\sigma_a^2 = 49 v^2$, $\epsilon_1 = 6 \times 10^{-8}$, $\epsilon_2 = 6 \times 10^{-4}$, and $j = 1$. (b) $N_{01}/2h = 10^5 v^2$, $N_{02}/2h = 0.1 v^2$, $a = 2 v$, $\epsilon_1 = 6$, $\epsilon_2 = 6 \times 10^{-2}$, $\epsilon_3 = 6 \times 10^{-6}$, and $j = 3$.

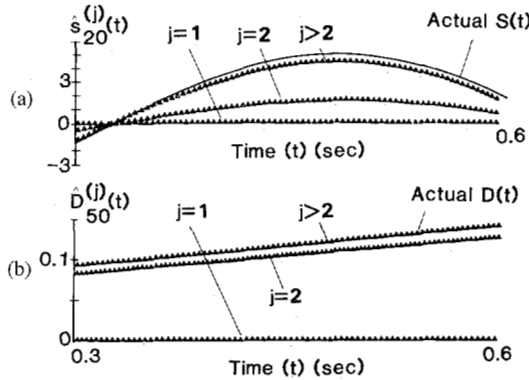


Fig. 17. Estimation of sinusoidal $s(t)$ and ramp $D(t)$ using Algorithm 2 with $N_{01}/2h = 100 v^2$, $N_{02}/2h = 0.01 v^2$, $a = 5 v$, $\sigma_a^2 = 49 v^2$, $b = 0.15$, $\sigma_b^2 = 0.05$, $h = 0.0031$ s, $\epsilon_1 = 6 \times 10^{-6}$, $\epsilon_2 = 6 \times 10^{-6}$, and $\epsilon_3 = 3 \times 10^{-6}$. (a) Actual $s(t)$ and its estimates. (b) Actual $D(t)$ and its estimates.

We can approximate $\partial/\partial \hat{a}_{n-1}(t) [E\{e^2(t)\}]$ by assuming that $E\{e^2(t)\}$ can be approximated by individual values of $e^2(t)$ [7].

Therefore,

$$\hat{a}_n(t) = \hat{a}_{n-1}(t) - \frac{\mu}{2} \frac{\partial}{\partial \hat{a}_{n-1}(t)} e^2(t). \quad (54)$$

Application of (52) in (54) yields

$$\hat{a}_n(t) = \hat{a}_{n-1}(t) + \mu \frac{\partial s(t, \hat{a}_{n-1}(t))}{\partial \hat{a}_{n-1}(t)} \cdot [s(t, a(t)) - s(t, \hat{a}_{n-1}(t))]. \quad (55)$$

Note that (55) is equivalent to (41) by assuming that

$$\begin{aligned} K_a(t, z) &= \frac{Q_o}{2} \delta(t - z) \\ n(t) &= 0 \\ \epsilon &= \frac{2N_o}{Q_o} \mu. \end{aligned} \quad (56)$$

In other words, assumptions (56) reduce the estimation based on ML criterion to the estimation based on MMSE criterion. It follows that for moderate noise environment ($n_2(t) \approx 0$)

$$\begin{aligned} \hat{D}_{m,j} &\approx \hat{D}_{m-1,j} - \mu_D \frac{\partial s(t_j - \hat{D}_{m-1,j})}{\partial (t_j - \hat{D}_{m-1,j})} \\ &\quad \cdot [r_2(t_j) - s(t_j - \hat{D}_{m-1,j})] \end{aligned} \quad (57)$$

where $\hat{D}_m(t_j) \triangleq \hat{D}_{m,j}$. Equation (57) is initialized with $\hat{D}_{0,0} = 0$, and then every point estimate be used to initiate the next point. That is, $\hat{D}_{0,j} = \hat{D}_{m,j-1}$ where $\hat{D}_{m,j-1}$ is the final estimate of $D(t_{j-1})$. This is depicted by the flow-chart shown by Fig. 18. The validity of this approach is illustrated by the following experiment.

Experiment 5: This experiment deals with a case for which $D(t)$, shown by Fig. 19(a), is a sample function from a Markov-1 process and the source signal is a known sinusoidal function with amplitude $5 v$ and radian frequency 5 . Fig. 20 illustrates estimation error, $e_d(t) = D(t) - \hat{D}(t)$, for $\rho = 0.95$, $\sigma_D^2 = 0.0026$ s², $h = 0.0063$ s, $N_{02}/2h = 10^2 v^2$, and $\mu_D = (32) \cdot 10^{-5}$.

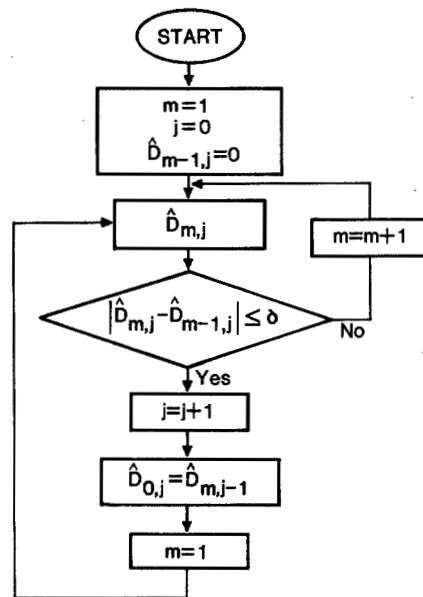
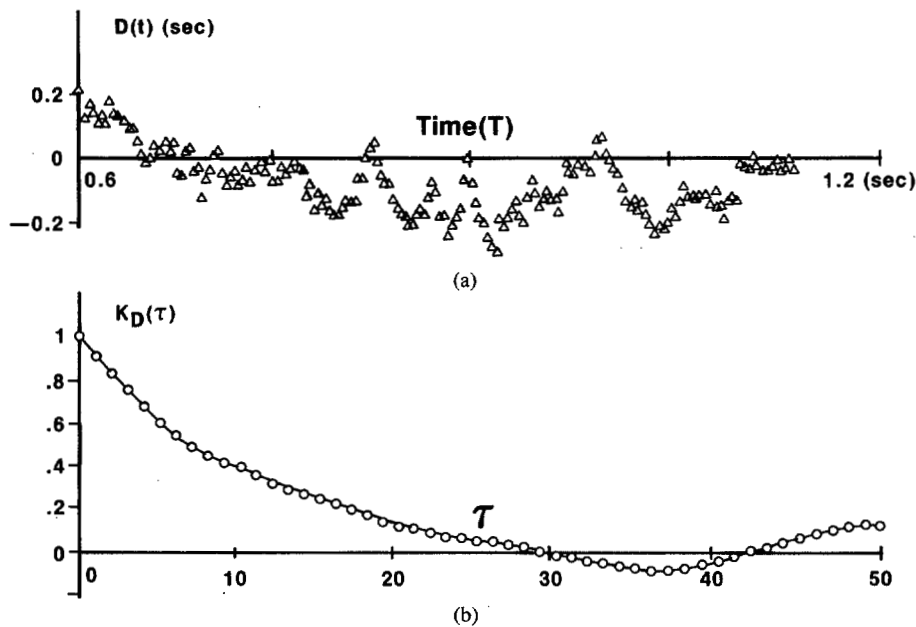
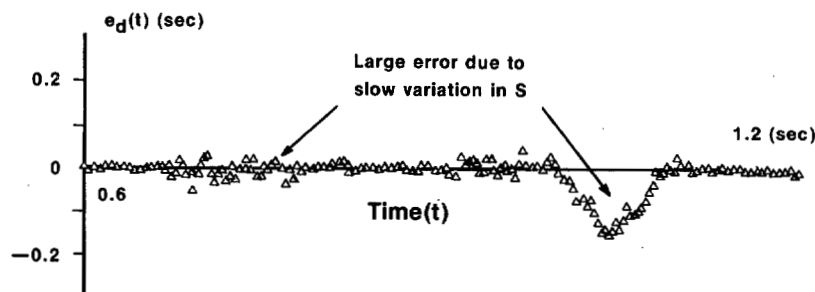


Fig. 18. Flowchart of algorithm used to solve (57).


 Fig. 19. (a) A sample function from the Markov-1 sequence generated by (48) with $\rho = 0.95$ and $\sigma_D^2 = 0.0026 \text{ s}^2$. (b) Estimate of normalized autocorrelation function of the process shown in (a).

 Fig. 20. Estimation error of the delay process shown in Fig. 19(a) using (57) with $N_{02}/2h = 0.01 \text{ v}^2$, $h = 0.0063 \text{ s}$, $a = 5 \text{ v}$, $w = 5 \text{ rad/s}$, and $\mu_D = (32) (10^{-5})$.

VIII. SUMMARY AND CONCLUSION

This paper has presented a new estimation algorithm for signal registration. The new algorithm was obtained by viewing the problem of signal registration as a demodulation problem.

We have developed a general recursive scheme from which a sequence of estimates $\{\hat{s}^{(1)}(t), \hat{D}^{(1)}(t), \hat{s}^{(2)}(t), \dots\}$ is generated, where $\hat{s}^{(1)}(t)$ is obtained using the noisier channel, and the rest of the estimates are conditionally obtained using the less contaminated received waveform. We have applied three criteria to our general scheme; namely, MAP, ML, and MMSE. Application of the MAP criterion resulted in Algorithm 1 whose validity was demonstrated by Experiments 1 and 2. Experiment 2 showed how the estimation scheme can be analytically designed for white delay ($K_D(t, z) = Q_o/2 \delta(t - z)$) and be used for nonwhite delay estimation. This is useful for the situations for which $s(t)$ is known and $K_D(t, z)$ is not known. Application of ML criterion along with a steepest ascent algorithm to our algorithm resulted in Algorithm 2. Although the integral equations (14) and (41) of the MAP and ML case were the same, the estimator based on ML criteria was found to be preferable due to the fact that its integral equations could be recursively solved with high degree of convergence.

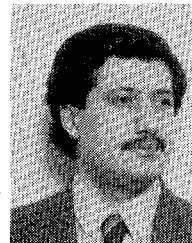
Finally, we obtain an estimator based on MMSE criterion and showed that it can be viewed as a special case of the ML estimator. The performance of this estimator was also examined by simulation experiment. Various simulations performed in this work demonstrated the ability of the proposed algorithms in dealing with variable delay in conjunction with a nonstationary source signal. However, more theoretical work is required to understand various aspects of the method including optimization, convergence, and performance.

ACKNOWLEDGMENT

The authors wish to thank the anonymous reviewers for their helpful comments.

REFERENCES

- [1] G. C. Carter, "Time delay estimation for passive sonar signal processing," *IEEE Trans. Acoust., Speech, Signal Processing*, vol. ASSP-29, pp. 463-470, June 1981.
- [2] A. N. Netravali and J. D. Robbins, "Motion-compensated television coding: Part I," *Bell Syst. Tech. J.*, vol. 58, no. 3, pp. 631-670, Mar. 1979.
- [3] Y. T. Chan, J. M. F. Riley, and J. B. Plant, "Modeling of time delay and its application to estimation of nonstationary delays," *IEEE Trans. Acoust., Speech, Signal Processing*, vol. ASSP-29, pp. 577-581, June 1981.
- [4] H. L. Van Trees, *Detection, Estimation, and Modulation Theory: Part I*. New York: Wiley, 1968.
- [5] M. Namazi, "A new approach to signal registration with the emphasis on variable time delay estimation," Ph.D. dissertation, Univ. Missouri-Rolla, Rolla, 1985.
- [6] F. Scheld, *Numerical Analysis*. New York: Schaum's Outline Series, 1968.
- [7] M. E. Etter and S. D. Stearns, "Adaptive estimation of time delays in sampled data systems," *IEEE Trans. Acoust., Speech, Signal Processing*, vol. ASSP-29, pp. 582-587, June 1981.
- [8] J. B. Cox, L. J. Hellums, T. J. Williams, R. S. Banks, and G. J. Kirk, "A practical spectrum of DDC chemical process control algorithms," *ISA-J.*, pp. 65-72, Oct. 1966.
- [9] J. A. Stuller, "Maximum likelihood estimation of time-varying delay—Part I," *IEEE Trans. Acoust., Speech, Signal Processing*, vol. ASSP-35, pp. 300-313, Mar. 1987.



Mohamad Namazi (S'84-M'85) was born in Tehran, Iran, on May 21, 1954. He received the Bachelor of Science degree in electrical engineering from Iran College of Science and Technology, Tehran, Iran, in 1977, and the Master of Science and Ph.D. degrees in electrical engineering from the University of Missouri-Rolla, Rolla, in 1981 and 1985, respectively.

He is presently an Assistant Professor of Electrical Engineering at Michigan Technological University, Houghton. His special fields of interest are signal processing and communications.

Dr. Namazi is a member of Sigma Xi.

John A. Stuller (SM'79), for a photograph and biography, see p. 313 of the March 1987 issue of this TRANSACTIONS.